Explorer

X-Ray Reflectivity and Grazing Incidence XRD

Introduction

Thin films are widespread in relevant fields such as optics, microelectronics, optoelectronics and hard coatings[1]. Thin films are quasi-two dimensional materials, where the third dimension (thickness) is greatly reduced in comparison with the other two and usually ranges from a few atomic layers to hundreds or thousands of nm. They have unique properties significantly different from the corresponding bulk materials as a result of their physical dimensions, geometry, non-equilibrium microstructure and metallurgy. They are strongly influenced by surface, interface effects and under intrinsic stress caused by lattice misfit with the substrate on which they are grown. Moreover, thin films are often used as a model material, due to the easy control of microstructure and possibility of applying several complementary characterization techniques.

X-Ray Reflectivity (XRR) and Grazing Incidence X-Ray Diffraction (GIXRD) are effective tools for the characterization of thin films and coatings, because they allow to get information on the parameters defining their functional properties.

XRR is based on the reflection and transmission of X-rays from surfaces and interfaces, occurring whenever there is a difference in the electron density between layers. XRR is used to estimate density, critical angle, layer thickness (ideally from 1 to 400 nm) and interface roughness of amorphous and crystalline thin film structures[2].

GIXRD is a closely related technique, which mainly consists in an asymmetric diffraction geometry, characterized by sequentially collecting radiation at different scattering angle (2θ) while keeping the incidence angle (ω) at a constant small value. This type of measurement is particularly useful in studying crystalline thin films grown on a substrate, whose contribution to the diffracted signal can overshadow that of the film of interest if a traditional symmetric ω–2θ or θ–θ scan is performed. The advantage of GIXRD is the reduced penetration of the beam into the substrate, thus minimizing its contribution to the scattered signal. Moreover planes with different orientation can be analyzed within one scan, in contrast to the symmetric geometry, in which only those parallel to the substrate can diffract[3].

Usually, some information about the deposited layers is available, so that the investigator can start the characterization with a model structure in mind.

Summary

Thin films are important technological materials characterized by peculiar properties related to their quasi-two dimensional structure. Their structural characterization by means of techniques at small angle of incidence, such as X-Ray Reflectivity and Grazing Incidence XRD, is of paramount importance in order to tailor them properly for the functional requirements of the high-tech industry. Explorer diffractometer, thanks to its parallel beam configuration and Mythen Hybrid Photon Counting linear detector, allows to perform these demanding measurements in an accurate and straightforward way.

[1] M. Ohring, Materials Science of Thin Films, 2nd edition 2002, Academic Press
[2] A. Gibaud and S. Hazra, CURRENT SCIENCE, VOL. 78, NO. 12, 25 JUNE 2000
[3] Mario Birkholz, Thin Film Analysis by X-Ray Scattering, WILEY-VCH

In order to investigate thin films at such small angles, both dedicated optical setup and mechanically precise sample stages are required on a diffractometer. Moreover, a detecting unit with a large dynamic range is mandatory in order to collect reflected photon fluxes spanning more than six orders of magnitude.
In this note, we will show how the Explorer diffractometer in parallel beam configuration allows to perform successfully XRR and GIXRD of thin films deposited on silicon substrates.

Theoretical overview

Refractive index *n* for X-Ray wavelengths is close to 1 and larger in vacuum (air) than in materials:

$$n = 1 - \delta - i\beta \qquad (1)$$

where

δ accounts for variation of the real part of the refractive index in the material;
β accounts for absorption in the material.

Recalling Snell's law and Fresnel's relations[4], there are both a reflected and a refracted beam each time an interface between two materials with different refractive index is present. The simplest case is when a single homogenous layer is on a substrate: the reflected wave amplitude at the air-film interface is the sum of the amplitudes of waves reflected and transmitted multiple times from the air-film and film-substrate interface. The phase difference of the waves is related to the thickness t of the film and the angle of incidence θ_i: by varying the incidence angle and thus the reflected one, the collected reflected intensity is characterized by oscillations (Kiessig fringes), with maxima occurring when the optical path difference of waves is an integer multiple of the radiation wavelength.

Maximum condition:

$$m2\pi = 2\pi/\lambda\,(\,2n_1 AB - n_{air} AC) + \psi$$

$$\psi = \begin{cases} 0 & n_1 > n_S \\ -\pi & n_1 < n_S \end{cases} \quad for\ S-pol.$$

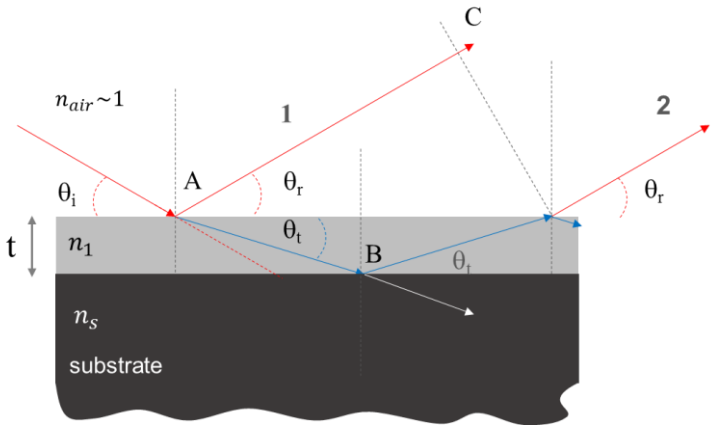

Basically, the closer the maxima are, the thicker the film is.
The ratio between the reflected intensity and the incident one is called reflectance (reflectivity). The profile of reflectance as a function of the incidence angle provides several information about the layer and its interfaces.

[4] M. Born and E. Wolf, Principles of Optics, 4th edition, Pergamon Press

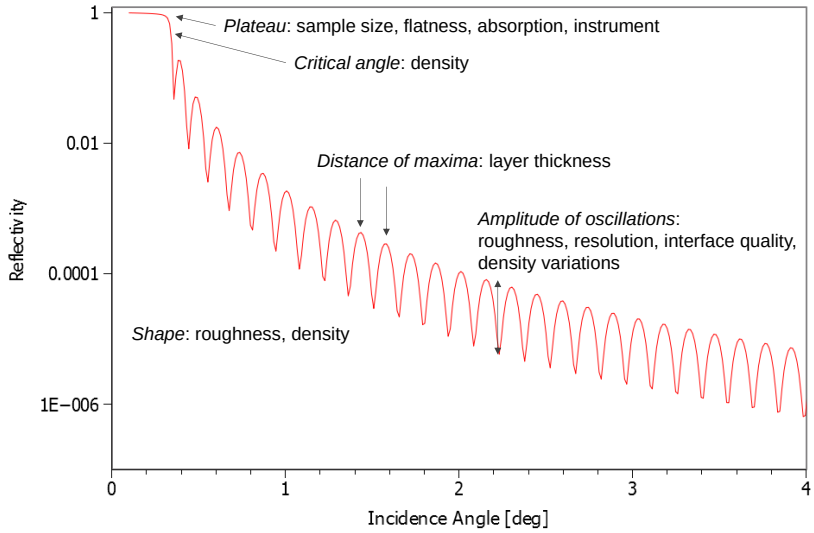

Despite some useful information can be retrieved by simply measuring the angular distance between maxima, usually computer simulations and fitting are carried out with algorithm implementing recursive application of Fresnel's relations[5].

It is possible to have no refraction and consequently complete reflection (total reflection) if the incidence angle is below the *critical* one (ω_c):

$$\omega_c[deg] = \sqrt{2\delta}\frac{180}{\pi} \qquad (2)$$

Typical values are reported in the following table for some materials Cu K_α radiation

Cu K_α (1.5418 Å)

	δ	β	ωc (deg)
Al	8.471 E-006	1.552 E-007	0.24
Si	7.5813432E-006	1.73066638E-007	0.22
Ti	1.352 E-005	1.136 E-006	0.30
Fe	2.246 E-005	2.901 E-006	0.38
Ni	2.43639515E-005	5.11858445E-007	0.40

Actually, not all the incoming radiation is reflected below the critical angle, because of absorption effects, given by the β parameter (eq. 1).

As far as crystalline films are concerned, it is possible to get diffraction signal from GIXRD analysis only if the incidence angle is larger than the critical one. Diffraction comes from planes of crystallites tilted with respect to the film surface, in order to satisfy Bragg's law.

The contribution to the diffracted signal detected at different scattering angles 2θ is a function of depth in the sample: the *penetration depth* (*63%)* gives the thickness of the sample from which 63% of the signal originates.

[5] IMD - Software for modeling the optical properties of multilayer films, D. L. Windt, Computers in Physics, 12, 360 (1998), http://www.rxollc.com/idl/index.html;

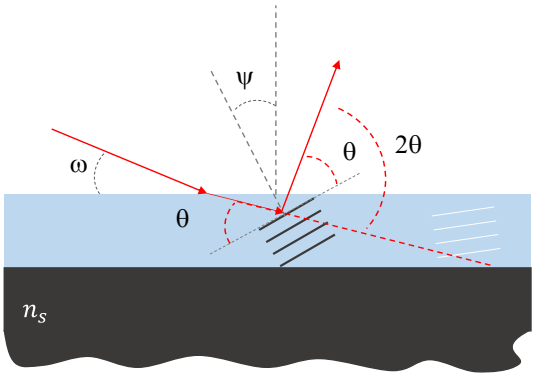

$$t_{63\%} = \frac{sin^2\theta - sin^2(\omega - \theta)}{2\mu \sin\theta \cos(\omega - \theta)} = \frac{sin^2\theta - sin^2\psi}{2\mu \sin\theta \cos\psi} \qquad (3)$$

where

$$\psi = \omega - \theta$$

$$\mu = \frac{4\pi\beta}{\lambda}$$

Working at small angles of incidence and discriminating fringes are demanding tasks.
For XRR, angular resolution depends on the emission spectrum of the X-ray source, the divergence angle of the incident beam and the aperture of the receiving slit: the capability of discriminating very close oscillation maxima allows to extend the upper limit for thickness quantification. A low background signal is important as well. Moreover, the beam height, i.e. equatorial dimension, should be limited, so that its projection at the critical angle is within the sample surface length. GIXRD capabilities are affected similarly and mostly by the asymmetric geometry setup.
The best solution for both techniques consists in a parabolic monochromator coupled with a long equatorial soller slit (LESS): the previous provides a quasi-parallel pure radiation (usually Cu K-α) with adjustable cross section, while the latter allows the detection of scattered radiation within a narrow angular range at each 2θ. For XRR, an additional receiving slit is mounted on LESS. Alternatively, a second parabolic mirror can replace LESS. A precise sample stage for film alignment is also required.

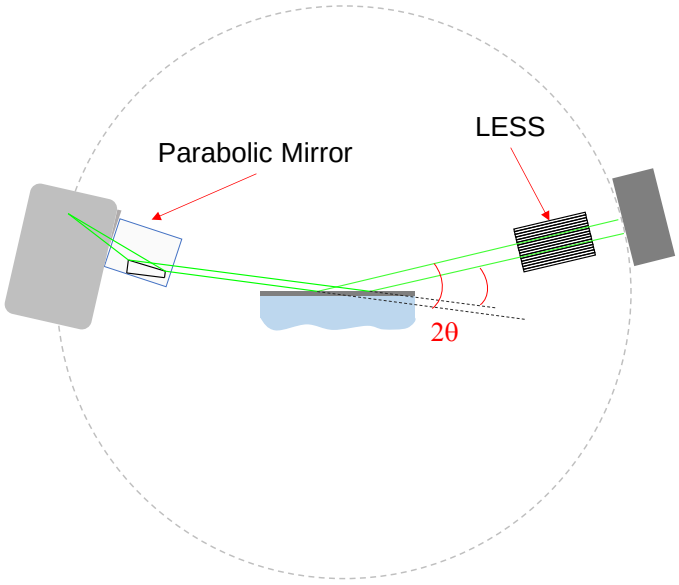

Product Specifications

Explorer is a Multi-Purpose Theta/Theta high resolution diffractometer which, thanks to its direct drive torque motors, offers top performances in many analytical areas, ranging from phase analysis to determination of microstructural properties on bulk or thin film materials.

Thanks to its modularity and the wide range of accessories and attachments available, Explorer allows to perform measurements in different configurations: traditional X-Ray Powder Diffraction (XRPD), Reflectometry (XRR), Grazing Incidence Diffraction (GID), High Resolution X-Ray Diffraction (HRXRD), Total Reflection X-Ray Fluorescence (TXRF), Residual Stress and Texture X-Ray Diffraction.

Explorer high resolution diffraction system incorporates the high efficiency of the direct drive torque motors controlled by optical encoders, allowing to reach an angular accuracy of 0.00001°.

The parallel beam setup features: parabolic monochromator, sample stage, LESS and linear detector, which is used in point mode.

ϕ rotation stage is mounted on a motorized z/Rx stage in order to position correctly the sample surface with respect to incident beam. ϕ with a range from 0 to 360 deg has a resolution better than 10^{-4} deg.

The z stage resolution is better than 0.005 mm, while the Rx one is better than 10^{-4} deg.

The allowed maximum sample diameter is about 120 mm, its height 20 mm while its max weight is up to 5 N.

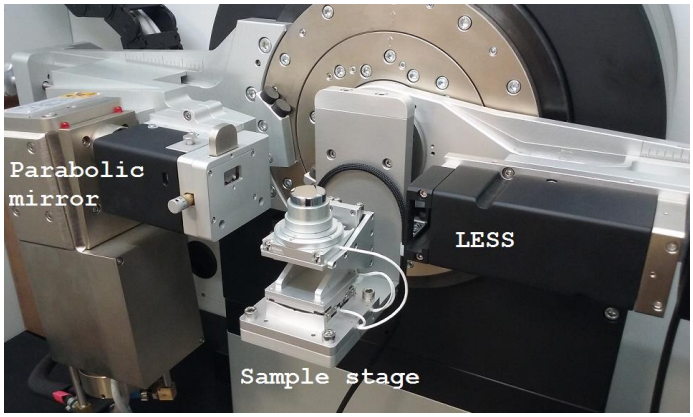

Experimental

Configuration:	Theta-Theta	LESS acceptance angle [deg]:	0.2
Goniometer radius [mm]:	240	Receiving slit (mm) (only XRR):	0.1
X-Ray Source:	Cu FF, Line focus	Detector:	MYTHEN 2 R 1D + attenuators
Power settings[kV, mA]	40, 30	Active area[°]:	2
Parabolic monochromator	Ni/C	Acquisition mode:	point mode scan
equatorial beam mask [mm]:	0.1		
axial beam mask [mm] [mm]:	8.0		

The analyzed samples are: one 30 nm thick Ni film and one periodic Ni/C multilayer (total thickness 70 nm) deposited on silicon, both provided by AXO Dresden. They can be attached to the sample holder by spreading a droplet of silicone oil on it just before placing the sample.
The measurable surface is 25.4 mm in diameter. With the optical setup chosen, the estimated beam projection on the sample at the critical angle is about 0.1/sin(0.4)=14.3 mm, so that it is completely within it.

Results

Nickel single layer on silicon substrate

First, the direct beam profile was collected in order to estimate the angular resolution provided by the optical setup[6]: with the receiving slit mounted, it was about 0.035 deg (2θ) in HWHM. Roughly, this accounts for the instrumental resolution function, whose convolution with the sample reflectivity profile gives the measured experimental one.

In order to figure out which angular step size is appropriate for the film under investigation, a simulation can be carried out with IMD software[5] by setting the proper instrumental function and known film parameters. Ideally, the 2θ step size should not be larger than one fifth of the angular distance between two consecutive minima. The simulation assesses also the fit for purpose of the optical setup, i.e. if the instrumental resolution and step size allow to distinguish Kiessig fringes.

Similar estimations can be done by calculating the expected angular positions of the first two maxima and minima (t=30 nm):

$$Maxima: \quad (\sin\theta_i)^2 = \left(\frac{\lambda}{2t}\right)^2 (m + 1/2)^2 + 2\delta \qquad m = 1, 2, 3, \ldots$$

$$Minima: \quad (\sin\theta_i)^2 = \left(\frac{\lambda}{4t}\right)^2 (n + 1)^2 + 2\delta \qquad n = 1, 3, 5, \ldots$$

t (nm)	ω_C (deg)	θ (n=1)	θ (n=3)	$\Delta 2\theta_{min}$ (deg)	$\Delta 2\theta_{min}$ /HWHM	θ (m=1)	θ (m=2)	$\Delta 2\theta_{MAX}$ /HWHM
30	0.40	0.43	0.50	0.14	~4	0.46	0.55	~5

The estimated minima separation is four times the HWHM of the instrumental function, thus the latter is well suited for the analysis. The same considerations apply to maxima separation. The chosen step size for 2θ was 0.01 degrees, even if twice that value would have been fine too for the current minima separation.

The ideal sample consists only of a silicon substrate and a Ni thin film, but actually one should expect the presence of additional layers, starting from the substrate: a thin native silicon oxide layer or a intermixed Ni-Si-O layer and a thin nickel oxide layer just on the top of the nickel one. Moreover, the roughness of each interface should be taken into account.

By inserting initial reasonable values in the simulation interface provided by IMD and then varying them to make the calculated profile resemble the experimental one, it is possible to have good starting values for the parameters to be refined. Both Levenberg-Marquardt and genetic algorithms are available. The fitted profile is reported in Figure 1, while results in Table 1. Note that reflectance is reported against the incidence angle, i.e. $2\theta/2$, after dividing the registered count rate by the direct beam one. The basic model's results are consistent with the manufacturer's ones. According to it, by refining additional parameters and even adding one more interface layer to the model, it would be possible to improve the matching with the experimental profile[7].

[6] A.Gibaud and G. Vignaud, Acta Cryst. (1993). A49, 642-648

[7] X-ray reflectometry teaching tool, Protocol, AXO Dresden

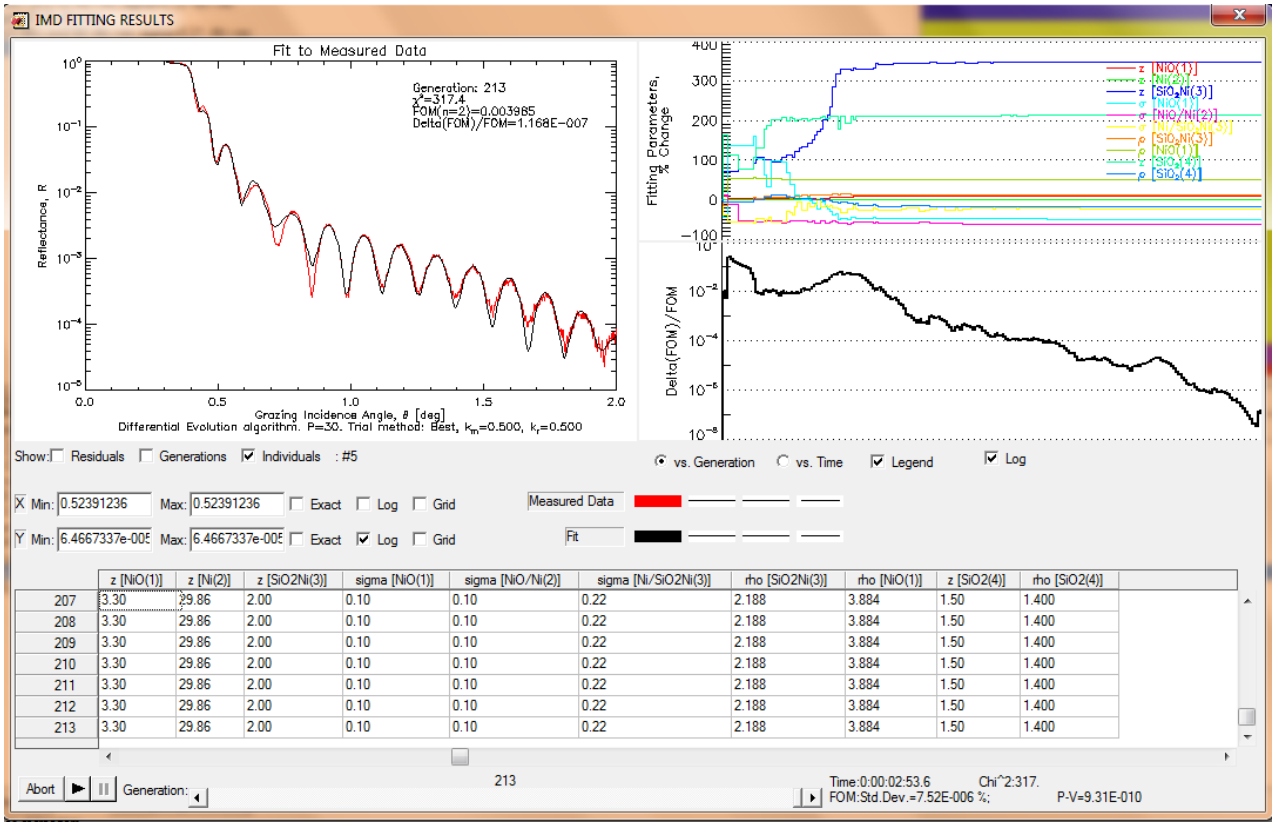

	z [NiO(1)]	z [Ni(2)]	z [SiO2Ni(3)]	sigma [NiO(1)]	sigma [NiO/Ni(2)]	sigma [Ni/SiO2Ni(3)]	rho [SiO2Ni(3)]	rho [NiO(1)]	z [SiO2(4)]	rho [SiO2(4)]
207	3.30	29.86	2.00	0.10	0.10	0.22	2.188	3.884	1.50	1.400
208	3.30	29.86	2.00	0.10	0.10	0.22	2.188	3.884	1.50	1.400
209	3.30	29.86	2.00	0.10	0.10	0.22	2.188	3.884	1.50	1.400
210	3.30	29.86	2.00	0.10	0.10	0.22	2.188	3.884	1.50	1.400
211	3.30	29.86	2.00	0.10	0.10	0.22	2.188	3.884	1.50	1.400
212	3.30	29.86	2.00	0.10	0.10	0.22	2.188	3.884	1.50	1.400
213	3.30	29.86	2.00	0.10	0.10	0.22	2.188	3.884	1.50	1.400

Figure 1. Reflectance pattern for Ni thin film on silicon substrate: experimental (red) and fitted (black) profiles. Note that half of 2θ is on x-axis.

Table 1. Results for Ni thin film on silicon substrate: basic model between parentheses.

	thickness (nm)	density (g/cm³)	roughness (nm)
Silicon substrate	--	2.2	0.15
SiO_2	1.50	1.4	--
	(2.00)	(1.6)	(0.38)
Si-O-Ni	2.00	2.2	0.22
	(--)	(--)	(--)
Ni	29.86	8.9	0.10
	(29.95)		(0.1)
NiO	3.30	3.9	0.10
	(3.10)	(3.7)	(0.1)

As regards Ni-phase XRD analysis, in order for the beam to cross the air-Ni interface, the angle of incidence must be larger than the critical one (eq. 2). The penetration depth (eq. 3) of a traditional symmetrical scan is more than 4 μm and increasing with scattering angle 2θ, while at a grazing angle of 0.9 deg the depth is about 300 nm and almost constant. Diffraction patterns are reported in Figure 2, where the outstanding detection capabilities of GIXRD are apparent. By using Scherrer's equation, the estimated apparent crystallite size for Ni is about 10 nm.

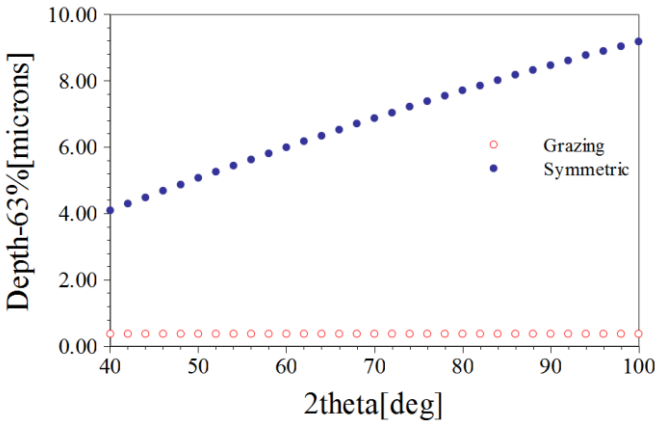

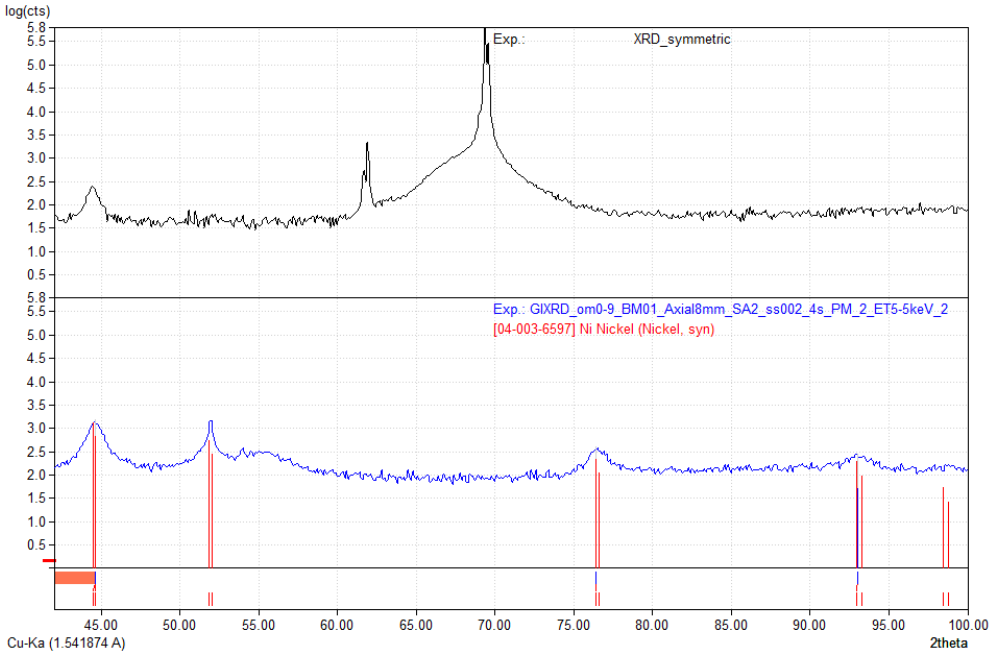

Figure 2. Symmetric (black) and GIXRD (blue) diffraction patterns: for the previous the silicon substrate (400) peak at about 69.4 deg. is overwhelmingly more intense than the Ni (111) one, while for the latter no strong signal from the substrate is present and more Ni planes are in diffracting conditions. Note that the y-scale is logarithmic for clarity.

Ni/C multilayer on silicon substrate

Periodic multilayer stacks can be used as monochromators in the hard and soft X-ray region.
The investigated one is:

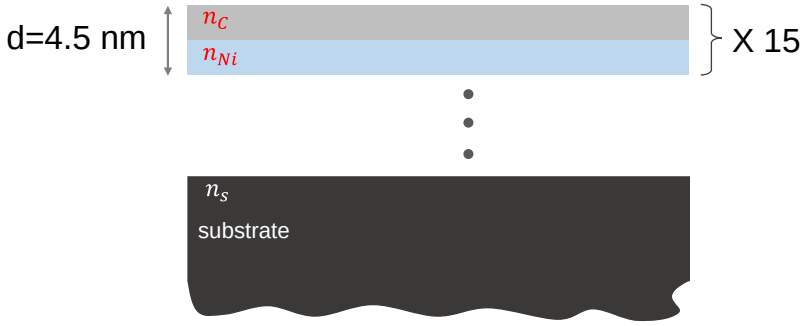

The repetition of Ni/C bilayer originates a reflectivity pattern characterized by two orders of oscillations: the small period ones are related to the kiessig fringes of the whole stack (~70 nm), while the ones characterized by intense peaks are related to Bragg's diffraction from the repeating unit (d=4.5 nm). In fact, peaks are found whenever:

$$2d \sin\theta = n\lambda$$

As done before, a rough estimation of maxima and minima separation can be carried out: while for Bragg's peaks the separation is 0.98 deg with a FWHM of 0.13 deg (Scherrer's formula), the high frequency oscillations are expected to be quite close, about 0.04 deg (in reality 0.06 deg).
The chosen step size for 2θ was again 0.01 degrees, in order to have a shorter acquisition time. Results are reported in Table 2 and Figure 3: even if the fit of the model is not perfect, the most important structural parameters are retrieved.

Table 2. Results for Ni/C multilayer.

	thickness (nm)	density (g/cm³)	roughness (nm)
Silicon substrate	--	2.2	0.05
SiO_2Ni	1.24	2.0	0.60
Ni (15x)	1.98	8.22	0.17
C (15x)	2.52	2.42	0.17 0.30 (top layer)

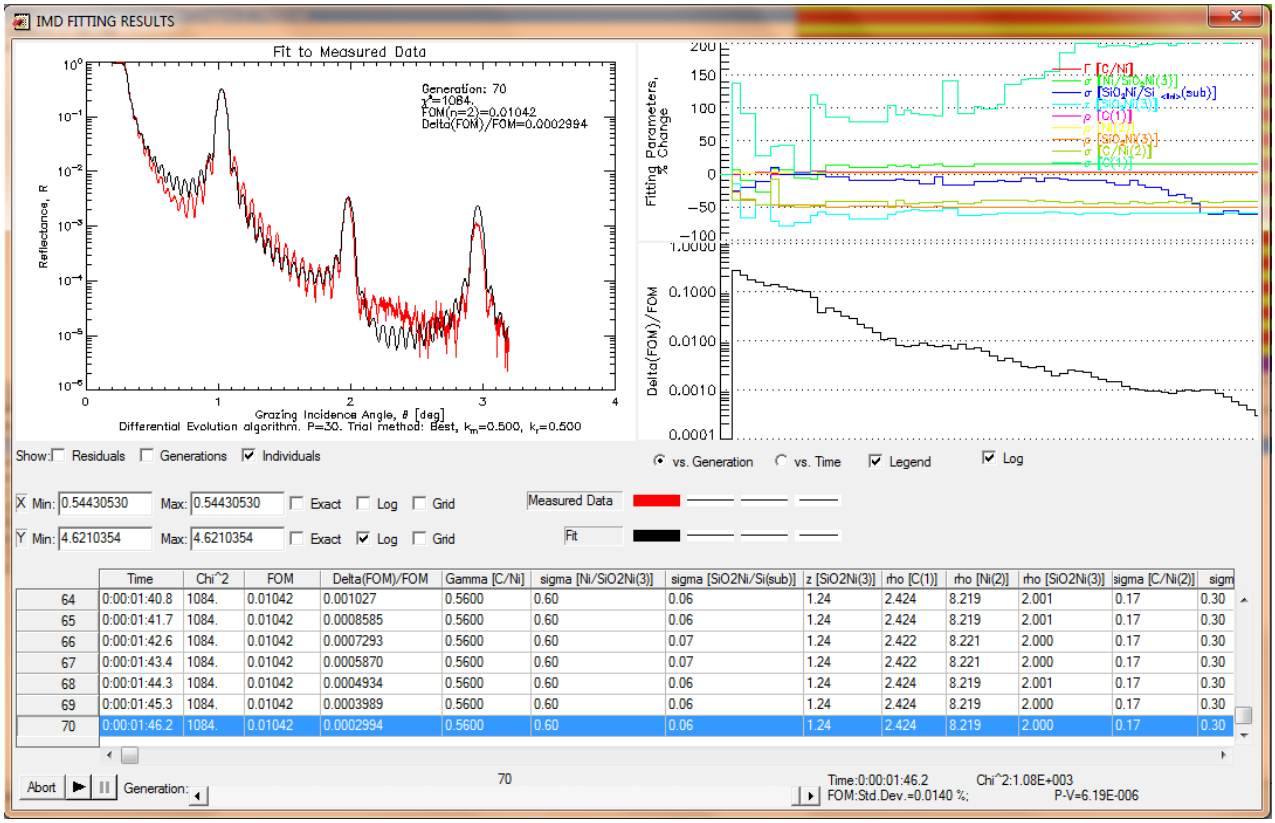

Figure 3. Reflectance pattern for Ni/C multilayer on silicon substrate: experimental (red) and fitted (black) profiles. Note that half of 2θ is on x-axis

Conclusions

Explorer, equipped with parabolic monochromator, equatorial soller slit and Mythen 2, allowed to perform successfully X-Ray Reflectivity and Grazing Incidence XRD on single layer and periodic thin films deposited by AXO Dresden company. The structural parameters determined through IMD software by fitting the model to the experimental data are in good agreement with the expected ones. X-Ray diffraction at grazing incidence detected crystalline cubic nickel phase on the single layer film.

Authors

Dr. Giacomo Siviero, X-Ray Product Specialist

About GNR SRL

With 35 years of technological experience, GNR is a worldwide market manufacturer of advanced analytical instruments in Optical Emission Spectrometer and XRD / XRF domain, developing procedures of analysis for various applications, supplying the corresponding laboratory equipment and providing consulting and customer support worldwide.

GNR can rely on a well-established team of highly qualified researchers and technicians, supported by the cooperation with leading University departments, which ensures a constantly updated technological growth.

GNR is present on the main international markets through an efficient and motivated technical and commercial network, able to provide outstanding support for any customer requirements.